

## Tunable Anti-Guiding Factor and Optical Gain of InGaAlAs/InP Nano-Heterostructure under Internal Strain

Pyare Lal<sup>1</sup>, Garima Bhardwaj<sup>2</sup>, Sandhya Kattayat<sup>3</sup>, P.A. Alvi<sup>1,\*</sup>

<sup>1</sup> Department of Physics, Banasthali Vidyapith-304022 Rajasthan, India

<sup>2</sup> Department of Electronics & Communication Engineering, IIMT Engineering College, Meerut-250001, UP, India

<sup>3</sup> Higher Colleges of Technology, Abu Dhabi, UAE

(Received 15 February 2020; revised manuscript received 10 April 2020; published online 25 April 2020)

This paper reports about the study of tunable anti-guiding factor and gain spectra of type-I GRIN (Graded Refractive Index) compressively strained InGaAlAs/InP nano-heterostructure. Through the modeling and mathematical simulation, the tuning behaviors of optical gain, differential gain and refractive index-change with carrier densities have been studied in the presence of internal strain which occurs due to lattice mismatch. According to the results, both the anti-guiding factor and optical gain are enhanced as increase in the percentage compressively strain. The lasing wavelength has also been found to shift towards lower values with increasing strain. These studies explain the tunability of the studied heterostructure and mostly utilized in optical fiber based communication systems.

**Keywords:** Anti-Guiding Factor, Optical gain, Differential gain, Current density

DOI: [10.21272/jnep.12\(2\).02002](https://doi.org/10.21272/jnep.12(2).02002)

PACS numbers: 42.55.Ah, 42.60.Lh, 73.21.Fg

### 1. INTRODUCTION

The III-V compound semiconducting materials such InGaAs, InAlAs, AlGaAs, GaAsSb, InGaAlAs etc have been reported as the potential candidates in the modern light-wave technologies having usage in manufacturing the photon emitting devices or radiations sensing devices [1-7]. In particular, the quaternary materials such as InGaAlAs nano-heterostructure have drawn a very high attention due to their emissions lying in the region of  $\sim 1.55 \mu\text{m}$  wavelength [8-12]. Actually, the radiations produced with such wavelengths are of most widely usage and, thus, have a variety of applications. Further, the optical sources like InGaAlAs/InP heterostructure with the release of  $1.55 \mu\text{m}$  radiations can often be preferred for optical broadcast due to eye protection issues. Though, a lot of study has been carried out on such material system, but still some more study is needed in context of some parametric relations. For example, gain vs compressive strain, optical wavelength vs compressive strain, differential gain vs carrier density are the relations of interest.

In the next sections of this article, a collective study of the optical gain characteristics in terms of wavelength taking into account the internal strain (compressive nature) that may occur due to lattice misalignment, the peak gain along with the optimized wavelength due to the compressive strains have been carried out. Furthermore, the refractive index profile as well as differential gain for different values of the compressive strain has also been analysed.

### 2. STRUCTURAL AND THEORITICAL DETAIL

The quaternary compound material i.e. InGaAlAs with the compositions of  $\text{In}_{0.71}\text{Ga}_{0.21}\text{Al}_{0.08}\text{As}$  having graded refractive index with the straddling nature has been utilized as an active region to design the heterostructure. The composition of the material is selected in

such a way so that desired wavelength corresponding to the peak gain could be achieved. The quantum well (thickness  $\sim 6 \text{ nm}$ ) of  $\text{In}_{0.71}\text{Ga}_{0.21}\text{Al}_{0.08}\text{As}$  is sandwiched in between twenty graded refractive index layers (thickness  $\sim 0.5 \text{ nm}$ ) of wide band gap material  $\text{In}_{0.41}\text{Ga}_{0.34}\text{Al}_{0.25}\text{As}$  (as a barrier) followed by cladding (thickness  $\sim 10 \text{ nm}$ ) of material  $\text{In}_{0.52}\text{Al}_{0.48}\text{As}$ . The whole structure is considered to be grown on InP substrate. Here, we have selected InP as a substrate because InP has a wider band gap as compared to the active layer and therefore has the advantage that a zero amount of radiative energy is absorbed inside the substrate region.

The optical gain for the studied device can be simulated with the following equation [12-14];

$$G(E) = \frac{q^2 |M_B|^2}{E \epsilon_0 m_0^2 c \hbar n_{\text{eff}} W} \sum_{i,j} \int_{E_g}^{E_{gb}} m_{r,ij} C_{ij} A_{ij} (f_c - f_v) L(E - E') dE'$$

The first differentiation of optical gain with respect to carrier density is referred as differential gain. The optical gain in terms of differential gain and carrier concentration is given by below relation:

$$G(N) = G'(N) \cdot [N - N_{tr}],$$

where  $G'(N)$  stands for differential gain,  $N$  and  $N_{tr}$  stand for carrier concentrations and transparency carrier densities. The relation between differential refractive index and differential gain is given by Anti-Guiding factor. The Anti-Guiding factor is expressed as below equation.

$$\alpha = 4\pi \cdot \left(\frac{1}{\lambda}\right) \cdot \left(-\frac{dn(E)}{dN}\right) \cdot \left(\frac{dG(E)}{dN}\right)^{-1},$$

where  $\lambda$  stands for wavelength of light propagation and the quantity  $dn(E)/dN$  stands for differential re-

\* [drpaalvi@gmail.com](mailto:drpaalvi@gmail.com)

fractive index with carrier concentrations; while the quantity  $dG(E)/dN$  stands for differential gain with carrier concentrations.

### 3. RESULTS AND THEIR PREDICTIONS

In general, the study of optical gain has an essential role in the realization of laser based on the semiconducting heterostructures [15, 16]. The optical gain provides a key role in the description of amplification of intensity of light in the semiconductor based materials [17, 18]. Basically, in the semiconducting heterostructures the optical gain occurs due to stimulated emission associated with the emission of light created by electron-hole recombination. In the semiconductors optical gain is caused by photon induced transition of electrons from the conduction band to valence sub bands. If the rate of down ward transitions surpasses the rate of upward transitions, there will be a net generation of photons and optical gain can be attained.

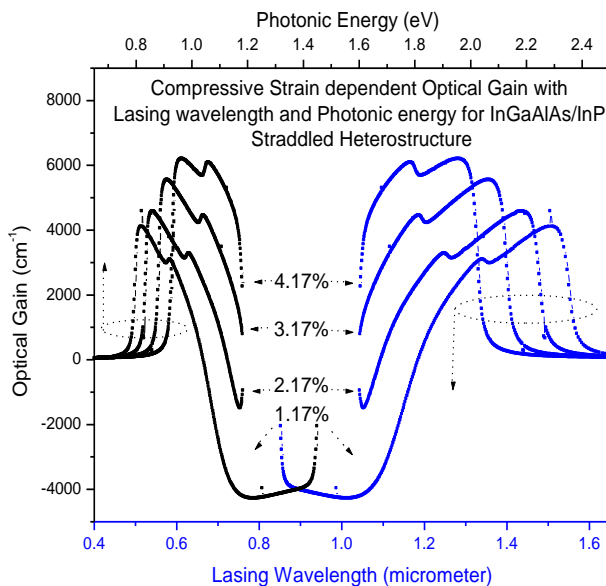


**Fig. 1** – Variations in optical gain with lasing wavelength and photonic energies for various percentage strains

In the nano scale heterostructures, the optical gain is measured in per centimetres because it is given by the enhancement in the intensity of light per unit originally intensity and per unit length.

The variations of optical gain with lasing wavelength is represented by left (y) and bottom (x) axes and variations of optical gain with photonic energies represented by by left (y) and top (x) axes for various percentage compressive strain of InGaAlAs/InP straddling type nano scale heterostructure in Fig. 1. It is clearly exhibited by Fig. 1 that the peak optical gains increase with increase in percentage compressive strain and the peaks of spectra are shifted towards lower values of lasing wavelength and higher values of photonic energies. The proportional behaviors of peak optical gain and inversely behaviors of lasing wave length with percentage compressive strain for InGaAlAs/InP straddling type nano scale heterostructure are shown by Fig. 2. In other words, Fig. 2 predicts that peak optical gain and peak gain wavelength (lasing wavelength)

play inversely behavior to each other. Moreover, for internal strain 4.17 %, the peak optical gain is found ~ 6200/cm at lasing wavelength ~ 1280 nm; for internal strain 3.17 %, the peak optical gain is found ~ 5800/cm at lasing wavelength ~ 1350 nm; for internal strain 2.17 %, the peak optical gain is found ~ 4700/cm at lasing wavelength ~ 1480 nm; and for internal strain 1.17 %, the peak optical gain is found ~ 4200/cm at lasing wavelength ~ 1550 nm. Hence this proposed heterostructure is more utilized in NIR radiation applications as well as optical fiber based communication systems due lowest optical losses [19, 20].

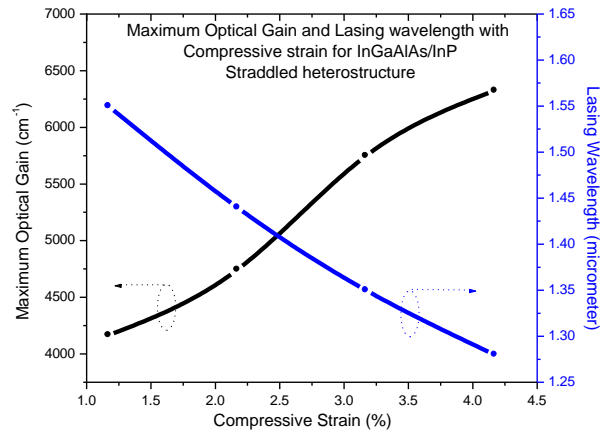


**Fig. 2** – Behaviors of peak (maximum) optical gain and lasing wavelength with percentage compressive strain

The index of refraction as well as dielectric constant depends on the charge carrier densities that is electrons and holes densities. In the semiconductor heterostructures devices, fluctuations in the carrier concentration affect both the optical differential gain and change in index of refraction. The behaviors of variations in index of refraction with current densities by left (y) and bottom (x) axes and behaviors of variations in differential gain with carrier densities by right (y) and top (x) axes for various percentage compressive strain of InGaAlAs/InP straddling type nano scale heterostructure are shown in Fig. 3. It is predicted by Fig. 3, that the differential gain has reciprocal proportional behavior with carrier densities. Next the maximum (peak) differential gain and saturated refractive index change both have proportional behavior with percentage internal strain.

It is very necessary to optimize the properties of device performance for accurate prediction of the optical gain and refractive index change in the semiconducting heterostructure. The coupling between optical gain and refractive index change induced by carrier concentration is termed as Anti-guiding factor. In other words the ratio of change in index of refraction per unit carrier concentration and change in optical gain per unit carrier concentration is called Anti-guiding factor. This type factor has crucial role in the prediction of beam quality of lasing devices and filamentation phenomena. In the heterostructure based lasers the Anti-Guiding factor provides substantial role as a crucial design parameter for high speed modulation. This type factor is a key parameter in the semiconductor lasing devices under continuous wave (CW) operation and high fre-

quency (HF) modulation. It can be characterized the line-width broadening due to fluctuation in the carrier concentrations altering the index of refraction. The behaviors of optical gain with current densities and range of Anti-Guiding factor with carrier densities by left (y) and bottom (x) axes and right (y) and top (x) axes respectively for various percentage compressive strain of InGaAlAs/InP straddling type nano scale heterostructure are shown in Fig. 4.

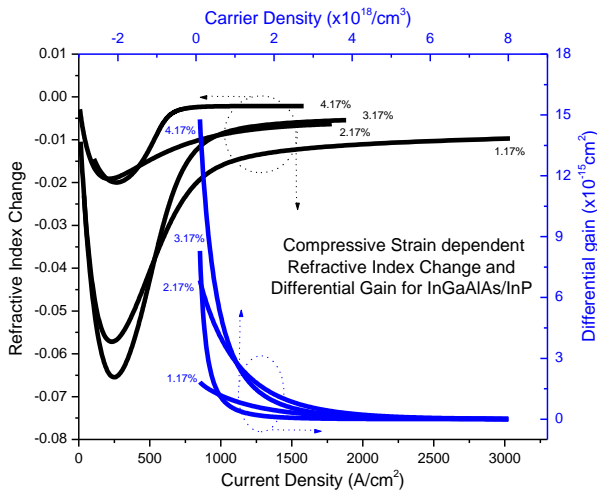


**Fig. 3** – Behaviors of change in index of refraction with current densities and variations in differential gain with carrier densities for various percentage strain (compressive)

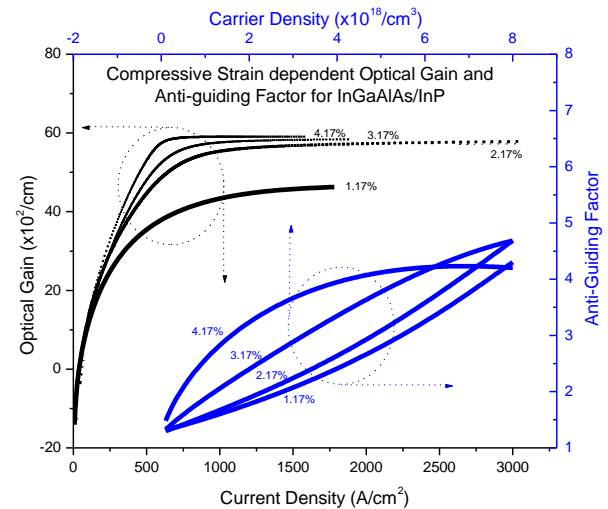


**Fig. 4** – Variations in optical gain with current densities and variations in Anti-Guiding factor with carrier densities for various percentage strain (compressive)

#### ACKNOWLEDGEMENTS

Authors are indebted to Banasthali Vidyapith for supporting the research facilities under CURIE project sanctioned by the DST, Government of India, New-Delhi.

#### REFERENCES

1. Pyare Lal, Shobhna Dixit, F. Rahman, P.A. Alvi, *Physica E* **46**, 224 (2012).
2. Pyare Lal, Rashmi Yadav, F. Rahman, P.A. Alvi, *Adv. Sci., Eng. Med.* **5** No 9, 918 (2013).
3. Xing Dai, Sen Zhang, Zilong Wang, Giorgio Adamo, Hai Liu, Yizhong Huang, Christophe Cousteau, Cesare Soci, *Nano Lett.* **14**, 2688 (2014).
4. P.A. Alvi, Pyare Lal, S. Dalela, M.J. Siddiqui, *Phys. Scripta* **85**, 035402 (2012).
5. P.A. Alvi, Pyare Lal, Rashmi Yadav, Shobhna Dixit, S. Dalela, *Superlattice. Microst.* **61**, 1 (2013).
6. Pyare Lal, Rashmi Yadav, Meha Sharma, F. Rahman, S. Dalela, P.A. Alvi, *Int. J. Mod. Phys. B* **28** No 29, 1450206 (2014).
7. H.K. Nirmal, Nisha Yadav, F. Rahman, P.A. Alvi, *Superlattice. Microst.* **88**, 154 (2015).
8. Sandra R. Selmic, Tso-Min Chou, Jieh Ping Sih, Jay B. Kirk, Art Mantle, Jerome K. Butler, David Bour, Gary A. Evans, *IEEE J. Sel. Top. Quant. Electron.* **7** No 2, 340 (2001).
9. O. Blum Sphan, T.-M. Chou, G.A. Evans, *Vertical-Cavity Surface-Emitting Laser Devices*, **6** (Springer Series in Photonics, Springer: Berlin, Heidelberg: 2003).
10. M. Kondow, T. Kitatani, S. Nakatsuka, M.C. Larson, K. Nakahara, Y. Yazawa, M. Okai, K. Uomi, *IEEE J. Sel. Top. Quant. Electron.* **3** No 3, 719 (1997).
11. M.O. Fischer, M. Reinhardt, A. Forchel, *IEEE J. Sel. Top. Quant. Electron.* **7** No 2, 149 (2001).
12. G. Morthier, R. Laroy, I. Christiaens, R. Todt, Th. Jacke, M.-C. Amann, J.-O. Wesstrom, S. Hammerfeldt, T. Mullane, N. Ryan, M. Todd, *Proc. SPIE* **5624** (2005).
13. Rashmi Yadav, Pyare Lal, F. Rahman, P.A. Alvi, *AIP Conf. Proc.* **1536**, 29 (2013).
14. Meha Sharma, Pyare Lal, M.J. Siddiqui, P.A. Alvi, *IEEE International Conference on Multimedia, Signal Processing and Communication Technologies (IMPACT)*, 283 (2013).
15. Z. Huang, M. Zimmer, S. Hepp, M. Jetter, P. Michler, *IEEE J. Quant. Electron.* **55** No 2, 2000307 (2019).
16. W.-M. Schulz, R. Roßbach, M. Reischle, G.J. Beirne, M. Bommer, M. Jetter, P. Michler, *Phys. Rev. B* **79** No 3, 035329 (2009).
17. G.M. Lewis, J. Lutti, P.M. Smowton, P. Blood, A.B. Krysa, S.L. Liew, *Appl. Phys. Lett.* **85**, 1904 (2004).
18. B.W. Hakki, T.L. Paoli, *J. Appl. Phys.* **46** No 3, 1299 (1975).
19. Satish Addanki, I.S. Amiri, P. Yupapin, *Result. Phys.* **10**, 743 (2018).
20. Sylvain Girard, Adriana Morana, Ayoub Ladaci, Thierry Robin, Luciano Mescia, Jean-Jacques Bonnefois, Mathieu Boutillier, Julien Mekki, Armelle Paveau, Benoît Cadier, *J. Opt.* **20**, 093001 (2018).